URL: http://dx.doi.org/10.1109/TSP.2011.2167613

Adaptive Detection of Distributed Targets in Compound-Gaussian Noise Without Secondary Data: A Bayesian Approach

Francesco Bandiera, *Member, IEEE*, Olivier Besson, *Senior Member, IEEE*, and Giuseppe Ricci, *Senior Member, IEEE*

***Abstract*—In this paper, we deal with the problem of adaptive detection of distributed targets embedded in colored noise modeled in terms of a compound-Gaussian process and without assuming that a set of secondary data is available. The covariance matrices of the data under test share a common structure while having different power levels. A Bayesian approach is proposed here, where the structure and possibly the power levels are assumed to be random, with appropriate distributions. Within this framework we propose GLRT-based and *ad-hoc* detectors. Some simulation studies are presented to illustrate the performances of the proposed algorithms. The analysis indicates that the Bayesian framework could be a viable means to alleviate the need for secondary data, a critical issue in heterogeneous scenarios.**

***Index Terms*—Adaptive detection, Bayesian detection, compound-Gaussian noise, distributed targets.**

I. Introduction

ADAPTIVE radar detection of multiple point-like or range-spread targets embedded in Gaussian disturbance has received an increasing attention from the radar community in recent years. In fact, the continuous advances of technology have made it possible to carry out radar systems with increased range resolution capabilities. In most cases the range resolution is much higher than the physical dimensions of the target to be detected. As a consequence of this, when a target is present in the illuminated area, it "appears" in more than one resolution cell. In addition, the traditional point-like target model can also fail when a low/medium resolution radar is used and the illuminated area is occupied, as an example, by a cluster of point-like targets moving at the same velocity and in spatial proximity to one another. Previously described scenarios require proper detection strategies taking into account at the design stage the distributed nature of the targets.

The associate editor coordinating the review of this manuscript and approving it for publication was Dr. Biao Chen. The work of O. Besson was supported by the Mission pour la Recherche et l'Innovation Scientifique (MRIS) of the DGA by Grant no. 2009.60.033.

F. Bandiera and G. Ricci are with the Dipartimento di Ingegneria dell'Innovazione, Università del Salento, 73100 Lecce, Italy (e-mail: francesco.bandiera@unisalento.it; giuseppe.ricci@unisalento.it).

O. Besson is with the Départment Electronique Optronique Signal, Université de Toulouse, ISAE, Toulouse Cedex 4, France (e-mail: olivier.besson@isae.fr).

Adaptive detection of distributed targets has been addressed in [1] and [2]; noise is modeled in terms of independent, complex normal random vectors with a common covariance matrix up to possibly different power levels. Covariance matrices are unknown at the receiver and a set of noise-only additional data (the so-called secondary data) is available for estimation purposes. In [2] detectors based on the generalized likelihood ratio test (GLRT) and ad hoc decision schemes (relying on the two-step GLRT-based design procedure) have been proposed for the case where noise vectors share one and the same covariance matrix (homogeneous scenario) or the same covariance matrix up to possibly different power levels between primary data, i.e., range cells under test, and secondary ones (partially homogeneous scenario). Proposed detectors possess the constant false alarm rate (CFAR) property under the design assumptions. Detection of distributed targets, modeled in terms of vectors confined to a known subspace, and embedded in unknown noise plus deterministic interference, has been considered in [3]–[5]. It is also worth pointing out that several detection algorithms are encompassed as special cases of the amazingly general framework and derivations in [1]. As to the statistical models for the noise components, experimental data [6]–[9] as well as physical and theoretical arguments [10], [11], have demonstrated that the Gaussian assumption is not always valid; in fact, the clutter can generally be modeled as a compound-Gaussian process that, when observed on sufficiently short time intervals, degenerates into a spherically invariant random process (SIRP) [12]–[14]. Relevant examples of detection algorithms for distributed targets embedded in non-Gaussian disturbance can be found in [15] and [16].

A fundamental assumption that all of the above papers share is that a set of secondary data, namely returns free of signals components, but sharing some characteristics with the data under test, is available. Such secondary data are usually used to come up with fully adaptive detection schemes. However, it has been evidenced that the homogeneous assumption for the secondary data is an idealized situation [17], [18], and that non-homogeneous environments are more commonly encountered. In order to mitigate the effects of nonhomogeneity, it is possible to select training samples that are most homogeneous with the cell under test and use only the retained ones to estimate the noise covariance matrix. The reader is referred to [19]–[23] for examples of applications of this rationale. These selection strategies result in significant performance improvement. However, they may require a large number of initial samples. The

assumption of secondary has been removed in [24] by using the "method of sieves," namely a modification of the GLRT. Such detector does not guarantee the CFAR property with respect to the covariance matrix of the noise vectors. CFAR detectors without assignment of a distinct set of secondary data have been recently proposed in [25] and [26], although at the price of a certain performance loss with respect to [24]. Another way to avoid the necessity of secondary data is to assume more structure on the noise. Examples of this modeling can be found in [27] and [28], where the noise is modeled as an autoregressive process and [29] where a more general state-space model is used for the noise.

Recently, the so-called knowledge-aided space-time adaptive processing (KA-STAP) has been recognized as one of the potentially most efficient way to handle heterogeneities [30]. KA-STAP improves the performance of adaptive detection schemes using additional (*a priori*) information, such as digital elevation and terrain data, synthetic aperture radar imagery, etc., [31], [32]. The reader is also referred to [33]–[39] for examples of application of such a rationale. Alternatively, a Bayesian approach can be advocated, as it is a relevant framework to handle uncertainties and to include *a priori* information. This framework allows to obtain a general and flexible, yet simple, model of nonhomogeneous environments, without very restrictive assumptions. Examples of this modeling can be found in [40]–[45]. The aforementioned works still assume that the secondary data samples are homogeneous with themselves; relevant exceptions are papers [44], [45]; more in detail, [44] extends the results of [43] to the case of heterogeneous samples assuming that the secondary data can be clustered in groups each one containing a certain number of snapshots with a common covariance matrix while [45] considers detection and estimation in a heterogeneous environment where secondary data have a common covariance structure and different power levels from one cell to another.

In this paper, using a Bayesian approach, we present detection algorithms for distributed targets embedded in non-Gaussian disturbance and without assuming that a set of secondary data is available. At the design stage we assume that a certain number of range cells is under test. Noise components in such cells are modeled as random vectors with a common structure and different power levels; both the structure and the power levels are modeled as random parameters with appropriate distributions. Within this framework we propose GLRT-based and *ad-hoc* detectors. Interestingly, some already proposed detectors can be envisaged as special cases of those herein derived. Finally, it is worth observing that some of the algorithms herein presented for the case of point-like targets have already been presented in [46].

The reminder of the paper is organized as follows: next section is devoted to the problem formulation and description of the data model while detector designs are the object of Section III. A performance assessment is presented in Section IV. Finally, some concluding remarks are given in Section V.

II. Problem Formulation

Assume that an array of N_a antennas senses K range cells and that each antenna collects N_t samples from each cell. Denote by $\boldsymbol{z}_k \in \mathbb{C}^{N\times 1}$, $k=1,\ldots,K$, the N-dimensional complex vector containing returns from the kth cell, with $N = N_a N_t$ and $\mathbb{C}$ being the complex field. We want to test whether or not the $\boldsymbol{z}_k$s contain useful signals backscattered from a range-spread target. The detection problem based upon such $\boldsymbol{z}_k$s can be formulated in terms of the following binary hypothesis test

$$\begin{cases} H_0 : \boldsymbol{z}_k = \boldsymbol{n}_k, & k=1,\ldots,K \\ H_1 : \boldsymbol{z}_k = \alpha_k \boldsymbol{v} + \boldsymbol{n}_k, & k=1,\ldots,K \end{cases} \tag{1}$$

where

- $\boldsymbol{v} \in \mathbb{C}^{N\times 1}$ is the *known* nominal steering vector;
- the α_ks are *unknown deterministic* complex scalars accounting for both channel and target effects;
- $\boldsymbol{n}_k \in \mathbb{C}^{N\times 1}$ is the additive noise term relative to the kth cell, $k=1,\ldots,K$.

As to the $\boldsymbol{n}_k$s, we use herein some variations on the well-known compound-Gaussian model. To be quantitative, recall that, in the compound-Gaussian case, the $\boldsymbol{n}_k$s can be written as

$$\boldsymbol{n}_k = \sqrt{\tau_k}\boldsymbol{g}_k, \quad k=1,\ldots,K \tag{2}$$

where, for each k, $\boldsymbol{g}_k$ is a complex normal random vector (the so-called speckle component) with zero mean and positive definite covariance matrix $\boldsymbol{R}$ and τ_k is a positive random variable (the so-called texture component). Moreover, we assume that the τ_ks and the $\boldsymbol{g}_k$s are each other independent. Based upon previous assumptions, it follows that, conditionally to the τ_ks and $\boldsymbol{R}$, the $\boldsymbol{n}_k$s are independent, zero-mean complex normal random vectors with covariance matrix $\tau_k\boldsymbol{R}$, in symbols

$$\boldsymbol{n}_k|\tau_k,\boldsymbol{R} \sim \mathcal{CN}_N(\boldsymbol{0},\tau_k\boldsymbol{R}), \quad k=1,\ldots,K. \tag{3}$$

Furthermore, in this paper we assume that $\boldsymbol{R}$ is a random quantity, too, independent of the τ_ks. More precisely, we assume that $\boldsymbol{R}$ is drawn from a complex inverse Wishart distribution, with *known* mean $\bar{\boldsymbol{R}}$ and $\nu\,(>N)$ degrees of freedom, i.e.

$$f(\boldsymbol{R}) = \frac{\left|(\nu-N)\bar{\boldsymbol{R}}\right|^{\nu}}{\tilde{\Gamma}_N(\nu)\,|\boldsymbol{R}|^{\nu+N}}\mathrm{etr}\left\{-(\nu-N)\boldsymbol{R}^{-1}\bar{\boldsymbol{R}}\right\} \tag{4}$$

where $|\cdot|$ is the determinant of the matrix argument, $\mathrm{etr}(\cdot)$ stands for the exponential of the trace of the matrix argument, and $\tilde{\Gamma}_N(\nu)$ is given by

$$\tilde{\Gamma}_N(\nu) = \pi^{\frac{N(N-1)}{2}}\prod_{n=1}^{N}\Gamma(\nu-n+1) \tag{5}$$

with $\Gamma(x)$ being, in turn, the Eulerian Gamma function. We denote as $\boldsymbol{R} \sim \mathcal{CW}^{-1}\left((\nu-N)\bar{\boldsymbol{R}},\nu\right)$ this distribution. It is worth highlighting the role of the parameters of the distribution. In fact, $\bar{\boldsymbol{R}}$ represents the expected value of $\boldsymbol{R}$ while ν sets the "distance" between $\bar{\boldsymbol{R}}$ and $\boldsymbol{R}$; as ν increases $\boldsymbol{R}$ is closer to $\bar{\boldsymbol{R}}$ (in the sense that the variance of $\boldsymbol{R}$ decreases). The role of $\bar{\boldsymbol{R}}$ can be interpreted as the *a priori* knowledge about the average covariance matrix. In practice, it can be obtained from the general clutter model introduced in [47], or by using some sample estimate of the covariance matrix from a very large window of data. As to the τ_ks, we use in this paper two different models

- the τ_ks are *unknown deterministic* parameters;

- the τ_ks are *independent random variables* ruled by the Gamma distribution, i.e.,

$$f(\tau_k)=\frac{\beta_k^{q_k}}{\Gamma(q_k)}\tau_k^{q_k-1}e^{-\beta_k\tau_k},\quad \tau_k\geq 0,\quad \beta_k>0,\quad q_k>0 \quad k=1,\ldots,K \tag{6}$$

which we denote as $\tau_k \sim \mathcal{G}(q_k,\beta_k)$. Notice that, conditioned on $\boldsymbol{R}$, the clutter is K-distributed if the τ_ks are Gamma distributed. It is also important to highlight the role of the (several) parameters of the model that eventually will enter the structure of the detectors. To this end, assume that the expected value of τ_k is equal to one, i.e., $E[\tau_k]=\frac{q_k}{\beta_k}=1$, which implies that $\beta_k=q_k$. Hence, the distribution of τ_k depends only on q_k; since, the smaller q_k, the larger the variance of τ_k, the q_ks can be used to fit the adopted model (and hence the detector's parameters) to the level of heterogeneity of the actual clutter data. Similar considerations apply to the choice of ν.

Some remarks about the chosen models are now in order. First, observe that a high resolution radar resolves an extended target in a certain number of scattering centers with unknown location. As a simplifying hypothesis, we have assumed that each cell contains a scatterer; the performance assessment (see Section V) will show that this approach provides good performances even under mismatched conditions. Second, the choice of an inverse Wishart for the distribution of $\boldsymbol{R}$ is mainly due to the fact that, since it is a conjugate prior, it is mathematically tractable. However, it is worth observing that such a choice is not completely far-fetched. Indeed, the inverse Wishart has already been used in other radar applications [41], [43] and it has provided good results also with real radar data [41]. It has also provided a rigorous and technically sound interpretation of the colored diagonal loading [48], [49] according to a Bayesian philosophy. Finally, the choice of a Gamma distribution for the τ_ks is widely accepted and verified, see, for instance, [6] and [8].

III. Detector Designs

For notational convenience, let us define the following arrays

$$\boldsymbol{Z}=[\boldsymbol{z}_1\cdots\boldsymbol{z}_K]\in\mathbb{C}^{N\times K} \tag{7}$$

$$\boldsymbol{\tau}=[\tau_1\cdots\tau_K]^T\in\mathbb{C}^{K\times 1} \tag{8}$$

$$\boldsymbol{\alpha}=[\alpha_1\cdots\alpha_K]^T\in\mathbb{C}^{K\times 1} \tag{9}$$

where the superscript ^{T} denotes transpose.

A. Deterministic τ_ks

The GLRT in this case can be written as

$$\frac{\max_{\boldsymbol{\tau}}\max_{\boldsymbol{\alpha}}\int f(\boldsymbol{Z};\boldsymbol{\alpha},\boldsymbol{\tau},\boldsymbol{R})f(\boldsymbol{R})d\boldsymbol{R}}{\max_{\boldsymbol{\tau}}\int f(\boldsymbol{Z};\boldsymbol{0},\boldsymbol{\tau},\boldsymbol{R})f(\boldsymbol{R})d\boldsymbol{R}}\underset{H_0}{\overset{H_1}{\gtrless}}\gamma \tag{10}$$

where $f(\boldsymbol{Z};i\boldsymbol{\alpha},\boldsymbol{\tau},\boldsymbol{R})$ denotes the probability density function (pdf) of $\boldsymbol{Z}$ under the H_i hypothesis, $i=0,1$, and γ is a proper threshold that ensures a preassigned probability of false alarm (P_{fa}). Based upon the models in force, it is readily verified that, for $i=0,1$

$$\begin{aligned} &f(\boldsymbol{Z};i\boldsymbol{\alpha},\boldsymbol{\tau},\boldsymbol{R})\\ &=\prod_{k=1}^{K}\frac{1}{\pi^N\tau_k^N|\boldsymbol{R}|}\exp\left\{-\frac{(\boldsymbol{z}_k-i\alpha_k\boldsymbol{v})^\dagger\boldsymbol{R}^{-1}(\boldsymbol{z}_k-i\alpha_k\boldsymbol{v})}{\tau_k}\right\}\\ &\propto\frac{1}{|\boldsymbol{R}|^K|\boldsymbol{D}_\tau|^N}\operatorname{etr}\left\{-\boldsymbol{R}^{-1}\boldsymbol{Z}_i\boldsymbol{D}_\tau^{-1}\boldsymbol{Z}_i^\dagger\right\} \end{aligned} \tag{11}$$

where $\propto$ means "proportional to", the superscript † denotes conjugate transpose, $\boldsymbol{D}_\tau\in\mathbb{C}^{K\times K}$ is a diagonal matrix whose diagonal entries are $\tau_1,\ldots,\tau_K$, and $\boldsymbol{Z}_i=\boldsymbol{Z}-i\boldsymbol{v}\boldsymbol{\alpha}^T$.

Integration over $\boldsymbol{R}$ is easily accomplished using the fact that the inverse Wishart distribution is a conjugate prior. Thus, we have (12), shown at the bottom of the page. After some straightforward manipulations, the GLRT given by (10) can be rewritten as (13), shown at the bottom of the page. Optimization over $\boldsymbol{\alpha}$

$$\begin{aligned} f(\boldsymbol{Z};i\boldsymbol{\alpha},\boldsymbol{\tau})&=\int f(\boldsymbol{Z};i\boldsymbol{\alpha},\boldsymbol{\tau},\boldsymbol{R})f(\boldsymbol{R})d\boldsymbol{R}\\ &\propto\frac{1}{|\boldsymbol{D}_\tau|^N}\int\frac{1}{|\boldsymbol{R}|^{\nu+K+N}}\operatorname{etr}\left\{-\boldsymbol{R}^{-1}\left[\boldsymbol{Z}_i\boldsymbol{D}_\tau^{-1}\boldsymbol{Z}_i^\dagger+(\nu-N)\bar{\boldsymbol{R}}\right]\right\}d\boldsymbol{R}\\ &\propto\frac{1}{|\boldsymbol{D}_\tau|^N\left|\boldsymbol{Z}_i\boldsymbol{D}_\tau^{-1}\boldsymbol{Z}_i^\dagger+(\nu-N)\bar{\boldsymbol{R}}\right|^{\nu+K}}. \end{aligned} \tag{12}$$

$$\frac{\max_{\boldsymbol{\tau}}\max_{\boldsymbol{\alpha}}f(\boldsymbol{Z};\boldsymbol{\alpha},\boldsymbol{\tau})}{\max_{\boldsymbol{\tau}}f(\boldsymbol{Z};\boldsymbol{0},\boldsymbol{\tau})}=\frac{\max_{\boldsymbol{\tau}}\max_{\boldsymbol{\alpha}}|\boldsymbol{D}_\tau|^{\nu+K-N}\left|\boldsymbol{D}_\tau+(\nu-N)^{-1}\boldsymbol{Z}_1^\dagger\bar{\boldsymbol{R}}^{-1}\boldsymbol{Z}_1\right|^{-(\nu+K)}}{\max_{\boldsymbol{\tau}}|\boldsymbol{D}_\tau|^{\nu+K-N}\left|\boldsymbol{D}_\tau+(\nu-N)^{-1}\boldsymbol{Z}_0^\dagger\bar{\boldsymbol{R}}^{-1}\boldsymbol{Z}_0\right|^{-(\nu+K)}}\underset{H_0}{\overset{H_1}{\gtrless}}\gamma. \tag{13}$$

is well known (see [1] or [2], for instance) and the maximizer is given by

$$\hat{\boldsymbol{\alpha}}^T = \frac{\boldsymbol{v}^\dagger \bar{\boldsymbol{R}}^{-1} \boldsymbol{Z}}{\boldsymbol{v}^\dagger \bar{\boldsymbol{R}}^{-1} \boldsymbol{v}}. \tag{14}$$

Substituting (14) into the GLRT (13) we get

$$\frac{\max_{\boldsymbol{\tau}} f(\boldsymbol{Z}; \hat{\boldsymbol{\alpha}}, \boldsymbol{\tau})}{\max_{\boldsymbol{\tau}} f(\boldsymbol{Z}; \boldsymbol{0}, \boldsymbol{\tau})} = \frac{\max_{\boldsymbol{\tau}} |\boldsymbol{D}_\tau|^{\nu+K-N} |\boldsymbol{D}_\tau + \boldsymbol{A}_1|^{-(\nu+K)}}{\max_{\boldsymbol{\tau}} |\boldsymbol{D}_\tau|^{\nu+K-N} |\boldsymbol{D}_\tau + \boldsymbol{A}_0|^{-(\nu+K)}} \underset{H_0}{\overset{H_1}{\gtrless}} \gamma \tag{15}$$

where, for $i = 0, 1$

$$\boldsymbol{A}_i = (\nu - N)^{-1} \left(\boldsymbol{Z} - i \frac{\boldsymbol{v}\boldsymbol{v}^\dagger \bar{\boldsymbol{R}}^{-1} \boldsymbol{Z}}{\boldsymbol{v}^\dagger \bar{\boldsymbol{R}}^{-1} \boldsymbol{v}} \right)^\dagger \bar{\boldsymbol{R}}^{-1} \times \left(\boldsymbol{Z} - i \frac{\boldsymbol{v}\boldsymbol{v}^\dagger \bar{\boldsymbol{R}}^{-1} \boldsymbol{Z}}{\boldsymbol{v}^\dagger \bar{\boldsymbol{R}}^{-1} \boldsymbol{v}} \right). \tag{16}$$

In order to solve the optimization problems over $\boldsymbol{\tau}$, we can, equivalently, solve the problem of maximizing the functions

$$J_i(\boldsymbol{\tau}) = \ln \left(|\boldsymbol{D}_\tau|^{\nu+K-N} |\boldsymbol{D}_\tau + \boldsymbol{A}_i|^{-(\nu+K)} \right), \quad i = 0, 1. \tag{17}$$

By setting to zero the derivative of $J_i(\boldsymbol{\tau})$ with respect to τ_k, $k = 1, \ldots, K$, we get

$$\frac{\partial J_i(\boldsymbol{\tau})}{\partial \tau_k} = (\nu + K - N) \frac{1}{\tau_k} - (\nu + K) \left[(\boldsymbol{D}_\tau + \boldsymbol{A}_i)^{-1} \right]_{kk} = 0, \quad k = 1, \ldots, K, \quad i = 0, 1 \tag{18}$$

where the notation $[\cdot]_{kk}$ stands for the (k,k)th element of the matrix argument. From (18) we have the following implicit equation in τ_k:

$$\tau_k = \frac{\nu + K - N}{\nu + K} \times \frac{1}{\left[(\boldsymbol{D}_\tau + \boldsymbol{A}_i)^{-1} \right]_{kk}}, \quad k = 1, \ldots, K, \quad i = 0, 1. \tag{19}$$

In order to solve (19), it is possible to advocate an iterative procedure. In practice, since we have found that $\boldsymbol{\tau} = g(\boldsymbol{\tau}, \boldsymbol{Z})$, we can start with an initial value $\boldsymbol{\tau}(0)$ (with positive entries) and compute $\boldsymbol{\tau}(n+1) = g(\boldsymbol{\tau}(n), \boldsymbol{Z})$ until a preassigned stopping criterion is met, see also [50]–[53], for discussions about convergence of such procedures. Observe also that the iterations have to be applied twice: for $i = 0$ and $i = 1$. Finally, it is important to highlight that the estimate provided by (19) is always real and positive; in fact, recall that $\nu \geq N$ and that the diagonal entries of the inverse of a positive definite Hermitian matrix are real and positive. Let us denote by $\boldsymbol{D}^{\mathrm{ML}}_{\hat{\tau}|i}$ the diagonal matrix whose diagonal elements are the results of the iterative procedures, for $i = 0, 1$; the GLRT is thus given by

$$\frac{\left| \boldsymbol{D}^{\mathrm{ML}}_{\hat{\tau}|1} \right|^{\nu+K-N} \left| \boldsymbol{D}^{\mathrm{ML}}_{\hat{\tau}|1} + \boldsymbol{A}_1 \right|^{-(\nu+K)}}{\left| \boldsymbol{D}^{\mathrm{ML}}_{\hat{\tau}|0} \right|^{\nu+K-N} \left| \boldsymbol{D}^{\mathrm{ML}}_{\hat{\tau}|0} + \boldsymbol{A}_0 \right|^{-(\nu+K)}} \underset{H_0}{\overset{H_1}{\gtrless}} \gamma. \tag{20}$$

Since detector (20) has been obtained for the case of deterministic $\boldsymbol{\tau}$, it will be referred to in the following as GLRT.

We have already said that matrix $\bar{\boldsymbol{R}}$ represents a sort of prior knowledge on the disturbance characteristics. Another way to incorporate such a knowledge into a decision statistic is to use a two-step design procedure. Specifically, we first assume that the true covariance matrix $\boldsymbol{R}$ is known and derive the GLRT, subsequently we substitute $\boldsymbol{R}$ with $\bar{\boldsymbol{R}}$. The GLRT for known $\boldsymbol{R}$ and deterministic $\boldsymbol{\tau}$, which is formally given by

$$\frac{\max_{\boldsymbol{\tau}} \max_{\boldsymbol{\alpha}} f(\boldsymbol{Z}; \boldsymbol{\alpha}, \boldsymbol{\tau})}{\max_{\boldsymbol{\tau}} f(\boldsymbol{Z}; \boldsymbol{0}, \boldsymbol{\tau})} \underset{H_0}{\overset{H_1}{\gtrless}} \gamma \tag{21}$$

has already been derived in [15] and [16] and the corresponding decision rule is

$$\prod_{k=1}^{K} \frac{\boldsymbol{z}_k^\dagger \boldsymbol{R}^{-1} \boldsymbol{z}_k}{\boldsymbol{z}_k^\dagger \boldsymbol{R}^{-1} \boldsymbol{z}_k - \frac{|\boldsymbol{z}_k^\dagger \boldsymbol{R}^{-1} \boldsymbol{v}|^2}{\boldsymbol{v}^\dagger \boldsymbol{R}^{-1} \boldsymbol{v}}} \underset{H_0}{\overset{H_1}{\gtrless}} \gamma. \tag{22}$$

As aforementioned, the detector incorporating prior knowledge on $\boldsymbol{R}$ is obtained replacing $\boldsymbol{R}$ with $\bar{\boldsymbol{R}}$. The resulting test, that will be referred to in the following as GLRT-$\bar{\boldsymbol{R}}$, of course is given by

$$\prod_{k=1}^{K} \frac{\boldsymbol{z}_k^\dagger \bar{\boldsymbol{R}}^{-1} \boldsymbol{z}_k}{\boldsymbol{z}_k^\dagger \bar{\boldsymbol{R}}^{-1} \boldsymbol{z}_k - \frac{|\boldsymbol{z}_k^\dagger \bar{\boldsymbol{R}}^{-1} \boldsymbol{v}|^2}{\boldsymbol{v}^\dagger \bar{\boldsymbol{R}}^{-1} \boldsymbol{v}}} \underset{H_0}{\overset{H_1}{\gtrless}} \gamma. \tag{23}$$

It is instructive to study detectors (20) and (23) when only one range cell is under test, i.e., when $K = 1$. From (15) we have

$$\frac{\max_{\tau} \tau^{\nu+1-N} (\tau + a_1)^{-(\nu+1)}}{\max_{\tau} \tau^{\nu+1-N} (\tau + a_0)^{-(\nu+1)}} \underset{H_0}{\overset{H_1}{\gtrless}} \gamma \tag{24}$$

where, for $i = 0, 1$,

$$a_i = (\nu - N)^{-1} \left(\boldsymbol{z} - i \frac{\boldsymbol{v}\boldsymbol{v}^\dagger \bar{\boldsymbol{R}}^{-1} \boldsymbol{z}}{\boldsymbol{v}^\dagger \bar{\boldsymbol{R}}^{-1} \boldsymbol{v}} \right)^\dagger \bar{\boldsymbol{R}}^{-1} \times \left(\boldsymbol{z} - i \frac{\boldsymbol{v}\boldsymbol{v}^\dagger \bar{\boldsymbol{R}}^{-1} \boldsymbol{z}}{\boldsymbol{v}^\dagger \bar{\boldsymbol{R}}^{-1} \boldsymbol{v}} \right). \tag{25}$$

Observe also that, since we are working with $K = 1$, we have dropped any dependence on the range-cell index k. Using the fact that maxima over τ in (24) are achieved for $\tau = \frac{a_i(\nu+1-N)}{N}$, it follows that the GLRT is equivalent to

$$\frac{a_0}{a_1} = \frac{\boldsymbol{z}^\dagger \bar{\boldsymbol{R}}^{-1} \boldsymbol{z}}{\boldsymbol{z}^\dagger \bar{\boldsymbol{R}}^{-1} \boldsymbol{z} - \frac{|\boldsymbol{z}^\dagger \bar{\boldsymbol{R}}^{-1} \boldsymbol{v}|^2}{\boldsymbol{v}^\dagger \bar{\boldsymbol{R}}^{-1} \boldsymbol{v}}} \underset{H_0}{\overset{H_1}{\gtrless}} \gamma \tag{26}$$

which, in turn, is equivalent to

$$\frac{|\boldsymbol{z}^\dagger \bar{\boldsymbol{R}}^{-1} \boldsymbol{v}|^2}{(\boldsymbol{z}^\dagger \bar{\boldsymbol{R}}^{-1} \boldsymbol{z})(\boldsymbol{v}^\dagger \bar{\boldsymbol{R}}^{-1} \boldsymbol{v})} \underset{H_0}{\overset{H_1}{\gtrless}} \gamma. \tag{27}$$

Equation (27) is recognized as the normalized matched filter (NMF) [54] with $\boldsymbol{R}$ substituted for the *a priori* matrix $\bar{\boldsymbol{R}}$. Observe now that starting from (23) and assuming $K = 1$ we get

again detector (27). We thus conclude that for detection of a point-like target (i.e., $K = 1$) the two approaches coincide.

B. Random τ_ks

In this section, we study the case where the τ_ks are independent random variables ruled by the Gamma distribution. In principle, the GLRT would be

$$\frac{\max_{\boldsymbol{\alpha}} \int\int f(\boldsymbol{Z};\boldsymbol{\alpha},\boldsymbol{\tau},\boldsymbol{R}) f(\boldsymbol{\tau}) f(\boldsymbol{R}) d\boldsymbol{\tau} d\boldsymbol{R}}{\int\int f(\boldsymbol{Z};\boldsymbol{0},\boldsymbol{\tau},\boldsymbol{R}) f(\boldsymbol{\tau}) f(\boldsymbol{R}) d\boldsymbol{\tau} d\boldsymbol{R}} \underset{H_0}{\overset{H_1}{\gtrless}} \gamma \tag{28}$$

where $f(\boldsymbol{\tau})$ is the joint pdf of $\tau_1, \ldots, \tau_K$, i.e.

$$f(\boldsymbol{\tau}) = \prod_{k=1}^{K} \frac{\beta_k^{q_k}}{\Gamma(q_k)} \tau_k^{q_k - 1} e^{-\beta_k \tau_k}. \tag{29}$$

Unfortunately, such detector cannot be obtained in closed form, but for the special case $K = 1$ that will be presented later in this section. For this reason, we propose a detector based upon the MAP estimate of $\boldsymbol{\tau}$. To be quantitative, the proposed decision rule can be written as follows:

$$\frac{\max_{\boldsymbol{\tau}} \max_{\boldsymbol{\alpha}} \int f(\boldsymbol{Z};\boldsymbol{\alpha},\boldsymbol{\tau},\boldsymbol{R}) f(\boldsymbol{\tau}) f(\boldsymbol{R}) d\boldsymbol{R}}{\max_{\boldsymbol{\tau}} \int f(\boldsymbol{Z};\boldsymbol{0},\boldsymbol{\tau},\boldsymbol{R}) f(\boldsymbol{\tau}) f(\boldsymbol{R}) d\boldsymbol{R}} \underset{H_0}{\overset{H_1}{\gtrless}} \gamma. \tag{30}$$

Since $f(\boldsymbol{\tau})$ does not depend on $\boldsymbol{R}$ and $\boldsymbol{\alpha}$ we can carry out integration over $\boldsymbol{R}$ and maximization over $\boldsymbol{\alpha}$ by gathering results obtained in previous section. In symbols, the problem becomes

$$\frac{\max_{\boldsymbol{\tau}} f(\boldsymbol{Z};\hat{\boldsymbol{\alpha}},\boldsymbol{\tau}) f(\boldsymbol{\tau})}{\max_{\boldsymbol{\tau}} f(\boldsymbol{Z};\boldsymbol{0},\boldsymbol{\tau}) f(\boldsymbol{\tau})} \underset{H_0}{\overset{H_1}{\gtrless}} \gamma \tag{31}$$

where $\hat{\boldsymbol{\alpha}}$ is given by (14). Using also (15) and (29), detector (31) can be explicitly written as

$$\frac{\max_{\boldsymbol{\tau}} |\boldsymbol{D}_\tau|^{\nu+K-N} |\boldsymbol{D}_\tau + \boldsymbol{A}_1|^{-(\nu+K)} \prod_{k=1}^{K} \frac{\beta_k^{q_k}}{\Gamma(q_k)} \tau_k^{q_k-1} e^{-\beta_k \tau_k}}{\max_{\boldsymbol{\tau}} |\boldsymbol{D}_\tau|^{\nu+K-N} |\boldsymbol{D}_\tau + \boldsymbol{A}_0|^{-(\nu+K)} \prod_{k=1}^{K} \frac{\beta_k^{q_k}}{\Gamma(q_k)} \tau_k^{q_k-1} e^{-\beta_k \tau_k}} \underset{H_0}{\overset{H_1}{\gtrless}} \gamma. \tag{32}$$

Ignoring irrelevant constants and writing $|\boldsymbol{D}_\tau|$ in an explicit form, we come up with the following rule:

$$\frac{\max_{\boldsymbol{\tau}} |\boldsymbol{D}_\tau + \boldsymbol{A}_1|^{-(\nu+K)} \prod_{k=1}^{K} \tau_k^{\nu+K-N+q_k-1} e^{-\beta_k \tau_k}}{\max_{\boldsymbol{\tau}} |\boldsymbol{D}_\tau + \boldsymbol{A}_0|^{-(\nu+K)} \prod_{k=1}^{K} \tau_k^{\nu+K-N+q_k-1} e^{-\beta_k \tau_k}} \underset{H_0}{\overset{H_1}{\gtrless}} \gamma. \tag{33}$$

Maxima over $\boldsymbol{\tau}$ in (33) can be obtained (as we have done in previous section) defining the functions

$$H_i(\boldsymbol{\tau}) = \ln\left(|\boldsymbol{D}_\tau + \boldsymbol{A}_i|^{-(\nu+K)} \prod_{k=1}^{K} \tau_k^{\nu+K-N+q_k-1} e^{-\beta_k \tau_k} \right), \quad i = 0, 1 \tag{34}$$

and setting to zero their derivatives for $k = 1, \ldots, K$

$$\frac{\partial H_i(\boldsymbol{\tau})}{\partial \tau_k} = -(\nu+K) \left[(\boldsymbol{D}_\tau + \boldsymbol{A}_i)^{-1} \right]_{kk} + \frac{(\nu + K - N + q_k - 1)}{\tau_k} - \beta_k = 0. \tag{35}$$

This provides the following set of implicit equations:

$$\tau_k = \frac{\nu + K - N + q_k - 1}{\beta_k + (\nu+K) \left[(\boldsymbol{D}_\tau + \boldsymbol{A}_i)^{-1} \right]_{kk}}, \quad k = 1, \ldots, K, \quad i = 0, 1 \tag{36}$$

that can be solved using again an iterative procedure. To come up with a final expression for the detector, let us denote by $\hat{\boldsymbol{D}}_{\tau|i}^{\mathrm{MAP}}$ the diagonal matrix whose diagonal elements, $\hat{\tau}_{k|i}^{\mathrm{MAP}}$ say, are the results of the iterative procedures, for $i = 0, 1$; the detector is thus given by

$$\frac{\left| \boldsymbol{D}_{\hat{\tau}|1}^{\mathrm{MAP}} + \boldsymbol{A}_1 \right|^{-(\nu+K)} \prod_{k=1}^{K} \left(\hat{\tau}_{k|1}^{\mathrm{MAP}} \right)^{\nu+K-N+q_k-1} e^{-\beta_k \hat{\tau}_{k|1}^{\mathrm{MAP}}}}{\left| \boldsymbol{D}_{\hat{\tau}|0}^{\mathrm{MAP}} + \boldsymbol{A}_0 \right|^{-(\nu+K)} \prod_{k=1}^{K} \left(\hat{\tau}_{k|0}^{\mathrm{MAP}} \right)^{\nu+K-N+q_k-1} e^{-\beta_k \hat{\tau}_{k|0}^{\mathrm{MAP}}}} \underset{H_0}{\overset{H_1}{\gtrless}} \gamma. \tag{37}$$

Since detector (37) has been obtained for the case of random $\boldsymbol{\tau}$ and MAP estimation, it will be referred to in the following as MAP-GLRT.

Let us turn now on the derivation of the detector for known $\boldsymbol{R}$. In this case it is possible to solve the GLRT

$$\frac{\max_{\boldsymbol{\alpha}} \int f(\boldsymbol{Z};\boldsymbol{\alpha},\boldsymbol{\tau}) f(\boldsymbol{\tau}) d\boldsymbol{\tau}}{\int f(\boldsymbol{Z};\boldsymbol{0},\boldsymbol{\tau}) f(\boldsymbol{\tau}) d\boldsymbol{\tau}} \underset{H_0}{\overset{H_1}{\gtrless}} \gamma. \tag{38}$$

The first step is again optimization over $\boldsymbol{\alpha}$. Following the lead of [2], we have that

$$\hat{\boldsymbol{\alpha}}^T = \frac{\boldsymbol{v}^\dagger \boldsymbol{R}^{-1} \boldsymbol{Z}}{\boldsymbol{v}^\dagger \boldsymbol{R}^{-1} \boldsymbol{v}}. \tag{39}$$

Observe that (39) and (14) are similar but not identical. In fact, they differ for the fact that (14) uses $\bar{\boldsymbol{R}}$ while (39) uses $\boldsymbol{R}$. Substituting (39) into the right-hand side (RHS) of the pdf (11) we get

$$f(\boldsymbol{Z}; i\hat{\boldsymbol{\alpha}}, \boldsymbol{\tau}) \propto \frac{1}{|\boldsymbol{R}|^K |\boldsymbol{D}_\tau|^N} \operatorname{etr}\left\{ -\boldsymbol{R}^{-1} \tilde{\boldsymbol{Z}}_i \boldsymbol{D}_\tau^{-1} \tilde{\boldsymbol{Z}}_i^\dagger \right\} \tag{40}$$

where

$$\tilde{\boldsymbol{Z}}_i = \boldsymbol{Z} - i\boldsymbol{v}\hat{\boldsymbol{\alpha}}^T, \quad i = 0, 1. \tag{41}$$

Integration over $\boldsymbol{\tau}$ is obtained as follows: [see (42) at the bottom of the next page], where $K_\nu(z)$ denotes the modified Bessel K function of order ν [55, par. 3.471]. Ignoring irrelevant constants and computing the ratio we get

(43), shown at the bottom of the page. Finally, we replace the true matrix $\boldsymbol{R}$ with $\bar{\boldsymbol{R}}$ into (43); the result is of course given by (44) at the bottom of the page, where $\hat{\alpha}_k$, $k = 1, \ldots, K$, has to be computed with $\bar{\boldsymbol{R}}$ in place of $\boldsymbol{R}$, i.e.,

$$\hat{\alpha}_k = \frac{\boldsymbol{v}^\dagger \bar{\boldsymbol{R}}^{-1} \boldsymbol{z}_k}{\boldsymbol{v}^\dagger \bar{\boldsymbol{R}}^{-1} \boldsymbol{v}}. \tag{45}$$

Detector (44) will be referred to in the following as GLRT-$\bar{\boldsymbol{R}}$-r. It can be viewed as a generalization of a previously derived scheme designed to detect point-like targets. In fact, when we consider the case of a single cell under test ($K = 1$), we get (46) at the bottom of the page, which has already been derived in [56].

Let us now turn back to test (28) and solve it for the special case of $K = 1$:

$$\frac{\max\limits_{\alpha} \int\int f(\boldsymbol{z}; \alpha, \tau, \boldsymbol{R}) f(\tau) f(\boldsymbol{R}) d\tau d\boldsymbol{R}}{\int\int f(\boldsymbol{z}; 0, \tau, \boldsymbol{R}) f(\tau) f(\boldsymbol{R}) d\tau d\boldsymbol{R}} \underset{H_0}{\overset{H_1}{\gtrless}} \gamma. \tag{47}$$

Based upon the assumptions made on $\boldsymbol{z}$, τ, and $\boldsymbol{R}$, it is promptly verified that, for $i = 0, 1$

$$f(\boldsymbol{z}; i\alpha, \tau, \boldsymbol{R}) = \frac{1}{\pi^N \tau^N |\boldsymbol{R}|} \exp\left\{ -\frac{(\boldsymbol{z} - i\alpha\boldsymbol{v})^\dagger \boldsymbol{R}^{-1} (\boldsymbol{z} - i\alpha\boldsymbol{v})}{\tau} \right\}. \tag{48}$$

Integration over $\boldsymbol{R}$ can be easily accomplished and we obtain (49) at the bottom of the page. The GLRT at this intermediate

$$\begin{aligned} f(\boldsymbol{Z}; i\hat{\boldsymbol{\alpha}}) &\propto \frac{1}{|\boldsymbol{R}|^K} \int \frac{1}{|\boldsymbol{D}_\tau|^N} \mathrm{etr}\left\{ -\boldsymbol{R}^{-1} \tilde{\boldsymbol{Z}}_i \boldsymbol{D}_\tau^{-1} \tilde{\boldsymbol{Z}}_i^\dagger \right\} f(\boldsymbol{\tau}) d\boldsymbol{\tau} \\ &\propto \prod_{k=1}^{K} \int_0^{+\infty} \frac{1}{\tau_k^N} \exp\left\{ -\frac{(\boldsymbol{z}_k - i\hat{\alpha}_k \boldsymbol{v})^\dagger \boldsymbol{R}^{-1} (\boldsymbol{z}_k - i\hat{\alpha}_k \boldsymbol{v})}{\tau_k} \right\} \tau_k^{q_k - 1} e^{-\beta_k \tau_k} d\tau_k \\ &= \prod_{k=1}^{K} \int_0^{+\infty} \tau_k^{q_k - N - 1} \exp\left\{ -\frac{(\boldsymbol{z}_k - i\hat{\alpha}_k \boldsymbol{v})^\dagger \boldsymbol{R}^{-1} (\boldsymbol{z}_k - i\hat{\alpha}_k \boldsymbol{v})}{\tau_k} \right\} e^{-\beta_k \tau_k} d\tau_k \\ &\propto \prod_{k=1}^{K} \left[\frac{(\boldsymbol{z}_k - i\hat{\alpha}_k \boldsymbol{v})^\dagger \boldsymbol{R}^{-1} (\boldsymbol{z}_k - i\hat{\alpha}_k \boldsymbol{v})}{\beta_k} \right]^{\frac{q_k - N}{2}} \\ &\quad \times K_{q_k - N}\left(2\sqrt{\beta_k (\boldsymbol{z}_k - i\hat{\alpha}_k \boldsymbol{v})^\dagger \boldsymbol{R}^{-1} (\boldsymbol{z}_k - i\hat{\alpha}_k \boldsymbol{v})} \right) \end{aligned} \tag{42}$$

$$\prod_{k=1}^{K} \left[\frac{(\boldsymbol{z}_k - \hat{\alpha}_k \boldsymbol{v})^\dagger \boldsymbol{R}^{-1} (\boldsymbol{z}_k - \hat{\alpha}_k \boldsymbol{v})}{\boldsymbol{z}_k^\dagger \boldsymbol{R}^{-1} \boldsymbol{z}_k} \right]^{\frac{q_k - N}{2}} \frac{K_{q_k - N}\left(2\sqrt{\beta_k (\boldsymbol{z}_k - \hat{\alpha}_k \boldsymbol{v})^\dagger \boldsymbol{R}^{-1} (\boldsymbol{z}_k - \hat{\alpha}_k \boldsymbol{v})} \right)}{K_{q_k - N}\left(2\sqrt{\beta_k \boldsymbol{z}_k^\dagger \boldsymbol{R}^{-1} \boldsymbol{z}_k} \right)} \underset{H_0}{\overset{H_1}{\gtrless}} \gamma. \tag{43}$$

$$\prod_{k=1}^{K} \left[\frac{(\boldsymbol{z}_k - \hat{\alpha}_k \boldsymbol{v})^\dagger \bar{\boldsymbol{R}}^{-1} (\boldsymbol{z}_k - \hat{\alpha}_k \boldsymbol{v})}{\boldsymbol{z}_k^\dagger \bar{\boldsymbol{R}}^{-1} \boldsymbol{z}_k} \right]^{\frac{q_k - N}{2}} \frac{K_{q_k - N}\left(2\sqrt{\beta_k (\boldsymbol{z}_k - \hat{\alpha}_k \boldsymbol{v})^\dagger \bar{\boldsymbol{R}}^{-1} (\boldsymbol{z}_k - \hat{\alpha}_k \boldsymbol{v})} \right)}{K_{q_k - N}\left(2\sqrt{\beta_k \boldsymbol{z}_k^\dagger \bar{\boldsymbol{R}}^{-1} \boldsymbol{z}_k} \right)} \underset{H_0}{\overset{H_1}{\gtrless}} \gamma \tag{44}$$

$$\left[\frac{(\boldsymbol{z} - \hat{\alpha} \boldsymbol{v})^\dagger \bar{\boldsymbol{R}}^{-1} (\boldsymbol{z} - \hat{\alpha} \boldsymbol{v})}{\boldsymbol{z}^\dagger \bar{\boldsymbol{R}}^{-1} \boldsymbol{z}} \right]^{\frac{q - N}{2}} \frac{K_{q - N}\left(2\sqrt{\beta (\boldsymbol{z} - \hat{\alpha} \boldsymbol{v})^\dagger \bar{\boldsymbol{R}}^{-1} (\boldsymbol{z} - \hat{\alpha} \boldsymbol{v})} \right)}{K_{q - N}\left(2\sqrt{\beta \boldsymbol{z}^\dagger \bar{\boldsymbol{R}}^{-1} \boldsymbol{z}} \right)} \underset{H_0}{\overset{H_1}{\gtrless}} \gamma \tag{46}$$

$$\begin{aligned} f(\boldsymbol{z}; i\alpha, \tau) &\propto \frac{1}{\tau^N} \int \frac{1}{|\boldsymbol{R}|^{\nu + N + 1}} \mathrm{etr}\left\{ -\boldsymbol{R}^{-1} \left[(\nu - N) \bar{\boldsymbol{R}} + \frac{(\boldsymbol{z} - i\alpha\boldsymbol{v})(\boldsymbol{z} - i\alpha\boldsymbol{v})^\dagger}{\tau} \right] \right\} d\boldsymbol{R} \\ &\propto \frac{1}{\tau^N} \left| \left[(\nu - N) \bar{\boldsymbol{R}} + \frac{(\boldsymbol{z} - i\alpha\boldsymbol{v})(\boldsymbol{z} - i\alpha\boldsymbol{v})^\dagger}{\tau} \right] \right|^{-(\nu + 1)} \\ &\propto \frac{1}{\tau^N} \left[1 + \frac{1}{\tau(\nu - N)} (\boldsymbol{z} - i\alpha\boldsymbol{v})^\dagger \bar{\boldsymbol{R}}^{-1} (\boldsymbol{z} - i\alpha\boldsymbol{v}) \right]^{-(\nu + 1)}. \end{aligned} \tag{49}$$

stage can thus be written as

$$\frac{\max_{\alpha} \int f(\boldsymbol{z};\alpha,\tau) f(\tau) d\tau}{\int f(\boldsymbol{z};0,\tau) f(\tau) d\tau} \underset{H_0}{\overset{H_1}{\gtrless}} \gamma. \tag{50}$$

Maximization over α is straightforward and it leads to

$$\max_{\alpha} f(\boldsymbol{z};\alpha,\tau) \propto \frac{1}{\tau^N}\left[1+\frac{1}{\tau(\nu-N)}\left(\boldsymbol{z}^\dagger \bar{\boldsymbol{R}}^{-1}\boldsymbol{z} - \frac{|\boldsymbol{z}^\dagger \bar{\boldsymbol{R}}^{-1}\boldsymbol{v}|^2}{\boldsymbol{v}^\dagger \bar{\boldsymbol{R}}^{-1}\boldsymbol{v}}\right)\right]^{-(\nu+1)}. \tag{51}$$

Define now the quantity

$$y_i = \begin{cases} \boldsymbol{z}^\dagger \bar{\boldsymbol{R}}^{-1}\boldsymbol{z}, & i=0, \\ \boldsymbol{z}^\dagger \bar{\boldsymbol{R}}^{-1}\boldsymbol{z} - \dfrac{|\boldsymbol{z}^\dagger \bar{\boldsymbol{R}}^{-1}\boldsymbol{v}|^2}{\boldsymbol{v}^\dagger \bar{\boldsymbol{R}}^{-1}\boldsymbol{v}}, & i=1. \end{cases} \tag{52}$$

Under both hypotheses we are left with the integral

$$\begin{aligned} f(\boldsymbol{z};i\hat{\alpha}) &\propto \int_0^{+\infty} \frac{1}{\tau^N}\left[1+\frac{y_i}{\tau(\nu-N)}\right]^{-(\nu+1)} f(\tau) d\tau \\ &\propto \int_0^{+\infty} \tau^{q-N-1}\left[1+\frac{y_i}{\tau(\nu-N)}\right]^{-(\nu+1)} e^{-\beta\tau} d\tau \end{aligned} \tag{53}$$

which can be computed using [55, p. 365] and the result is

$$\begin{aligned} f(\boldsymbol{z};i\hat{\alpha}) \propto & \left(\frac{y_i}{\nu-N}\right)^{q-N} \\ & \times \Psi\left(q-N+\nu+1; q-N+1; \frac{\beta y_i}{\nu-N}\right) \end{aligned} \tag{54}$$

where $\Psi(a;b;z) = z^{-a}\,{}_2F_0(a,1+a-b;\,;-\frac{1}{z})$, and ${}_2F_0(\cdot,\cdot;\,;\cdot)$ is a hypergeometric function [57, p. 504]. Using [57, par. 13.1.7, pag. 504] we have

$$\begin{aligned} & \left(\frac{y_i}{\nu-N}\right)^{q-N} \Psi\left(q-N+\nu+1; q-N+1; \frac{\beta y_i}{\nu-N}\right) \\ & \qquad = \frac{1}{\beta^{q-N}} \Psi\left(\nu+1; N-q+1; \frac{\beta y_i}{\nu-N}\right) \end{aligned} \tag{55}$$

and the GLRT is finally given by

$$\frac{\Psi\left(\nu+1; N-q+1; \frac{\beta y_1}{\nu-N}\right)}{\Psi\left(\nu+1; N-q+1; \frac{\beta y_0}{\nu-N}\right)} \underset{H_0}{\overset{H_1}{\gtrless}} \gamma. \tag{56}$$

IV. Performance Assessment

In this section, we use standard Monte Carlo counting techniques to evaluate the performance of the proposed algorithms. Specifically, the analysis is carried out in two parts: we first analyze the detectors under the design assumptions; second, we conduct a study to quantify their sensitivity to possible mismatches between nominal and operating conditions.

A. Analysis Under Matched Conditions

In this section, we show that detectors derived modeling the structure of the covariance matrix in terms of an inverse Wishart distribution (i.e., GLRT and MAP-GLRT detectors) can outperform those obtained incorporating an average matrix (i.e., GLRT-$\bar{\boldsymbol{R}}$ and GLRT-$\bar{\boldsymbol{R}}$-r). Towards this end, we evaluate the probability of detection (P_d), i.e., the probability to decide for H_1 when it is actually in force, given P_{fa}. Data are generated according to the model described is Section II. More specifically, we set $N=8$, $\nu=10$, $q=q_1=\cdots=q_K$, $\beta=\beta_1=\cdots=\beta_K$, $q=\beta$. As to $\bar{\boldsymbol{R}}$, we assume an exponentially correlated covariance matrix with one-lag correlation coefficient $\rho=0.95$, i.e., the (i,j)th element of $\bar{\boldsymbol{R}}$ is given by $\rho^{|i-j|}$. Moreover, we set to 3 the number of iterations used by the estimators of $\boldsymbol{\tau}$ and we use the following values

$$\hat{\tau}_k(0) = \frac{1}{N}\boldsymbol{z}_k^\dagger \bar{\boldsymbol{R}}^{-1}\boldsymbol{z}_k, \quad k=1,\ldots,K, \tag{57}$$

as the starting points for the iterations. Finally, we assume that, under the H_1 hypothesis, all of the K cells under test contain a target scatterer with the same amplitude $A=|\alpha_k|$.

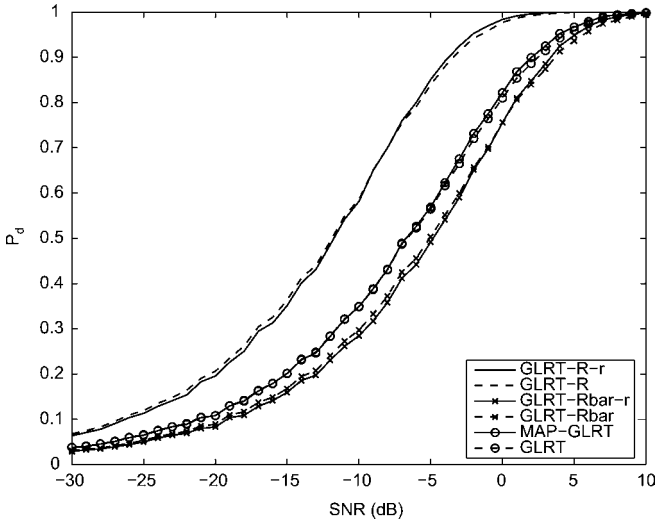

Fig. 1. P_d versus SNR for the considered detectors: $N=8$, $K=2$, $\nu=10$, $q=\beta=0.5$, $P_{fa}=10^{-3}$.

The overall signal-to-noise ratio (SNR) is defined as

$$\mathrm{SNR} = \frac{KA^2}{N}\boldsymbol{v}^\dagger \bar{\boldsymbol{R}}^{-1}\boldsymbol{v} \tag{58}$$

i.e., as the overall SNR after a whitening transformation. The P_{fa} is set to 10^{-3} and the corresponding thresholds are evaluated over $\frac{100}{P_{fa}}$ independent runs, while the P_ds are computed on 10^4 independent runs.

Figs. 1–3 refer to $q=0.5$ and K equal to 2, 8, 16, respectively, while Figs. 4 and 5 show results for $q=4$ and K equal to 8 and 16, respectively. For the sake of comparison, the performances of the GLRTs derived assuming that $\boldsymbol{R}$ is known (denoted by GLRT-$\boldsymbol{R}$ and GLRT-$\boldsymbol{R}$-r) are also given. All of the figures show that:

- GLRT and MAP-GLRT outperform GLRT-$\bar{\boldsymbol{R}}$ and GLRT-$\bar{\boldsymbol{R}}$-r, thus proving that information brought by the data can be efficiently combined with the prior information (on $\boldsymbol{R}$) in order to come up with better performance;
- the gain increases as K increases; the fact that the gain reduces as K decreases is not completely surprising since,

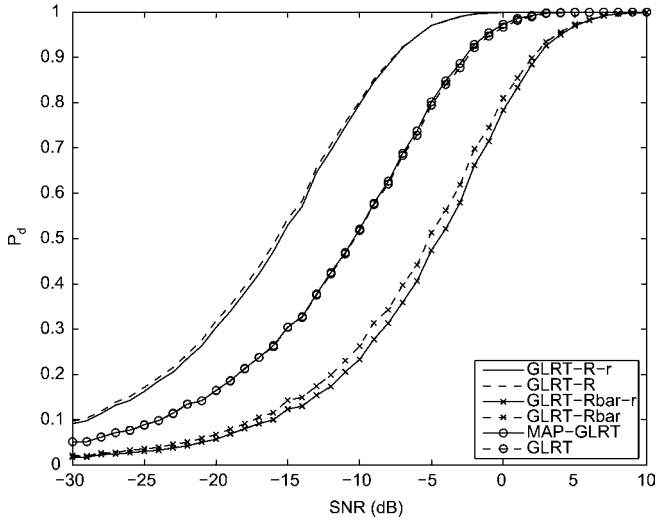

Fig. 2. P_d versus SNR for the considered detectors: $N = 8$, $K = 8$, $\nu = 10$, $q = \beta = 0.5$, $P_{fa} = 10^{-3}$.

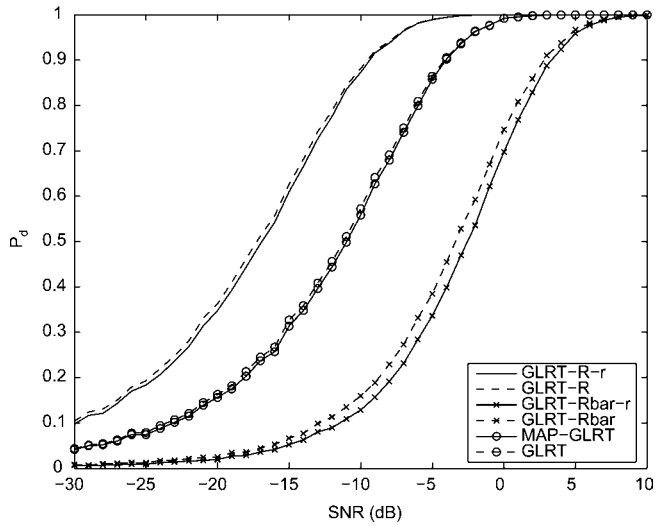

Fig. 3. P_d versus SNR for the considered detectors: $N = 8, K = 16, \nu = 10$, $q = \beta = 0.5$, $P_{fa} = 10^{-3}$.

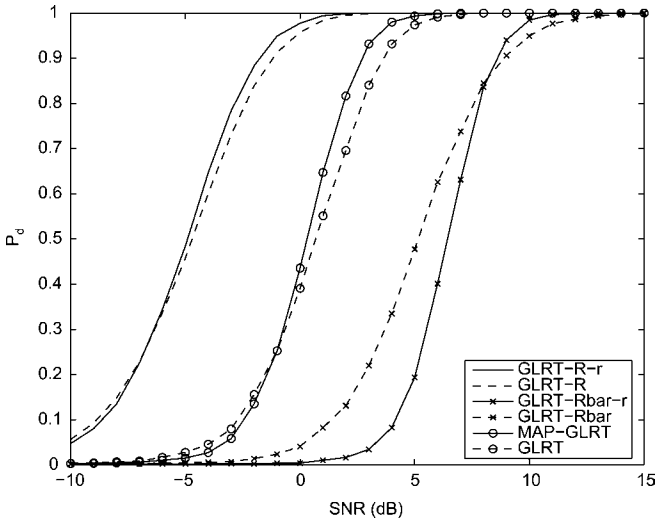

Fig. 4. P_d versus SNR for the considered detectors: $N = 8$, $K = 8$, $\nu = 10$, $q = \beta = 4$, $P_{fa} = 10^{-3}$.

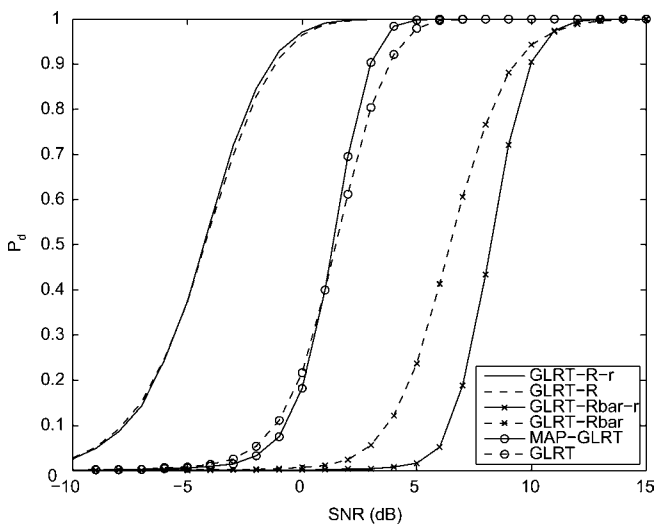

Fig. 5. P_d versus SNR for the considered detectors: $N = 8, K = 16, \nu = 10$, $q = \beta = 4$, $P_{fa} = 10^{-3}$.

as demonstrated in [46] for $K = 1$, the proposed clutter model is equivalent to a plain compound-Gaussian model with different pdf for the texture and nonrandom covariance matrix.

Notice also that GLRT and MAP-GLRT (GLRT-$\bar{\boldsymbol{R}}$ and GLRT-$\bar{\boldsymbol{R}}$-r as well) are practically equivalent for $q = 0.5$. On the other hand, Figs. 4 and 5 show that for $q = 4$ the MAP-GLRT is slightly better than the GLRT (for values of P_d greater than 0.5).

B. Sensitivity Analysis

We present in the sequel some sensitivity studies. To begin with, recall (see Section II) that a high resolution radar resolves an extended target in a certain number of scattering centers that are usually not contiguous along range while we have assumed at the design stage that all of the K cells contain a scatterer. For this reason, it is important to quantify the collapsing loss resulting from a sparse target. To this end, in Figs. 6 and 7 we plot the performance of the detectors when the actual number of cells occupied by the extended target, say N_t, is less than K; specifically, we set N_t equal to 2,4, and the remaining parameters as in Fig. 4. From the comparison of Figs. 4, 6, and 7, it is seen that a certain loss is experienced by all of the reported detectors; remarkably, the proposed detectors (i.e., those marked with "o" in the curves) generally experience a reduced loss with respect to detectors using $\bar{\boldsymbol{R}}$ in place of the true $\boldsymbol{R}$ (i.e., those marked with "x" in the curves).

We have also assessed the influence on the actual P_{fa} of possible mismatches between nominal and actual values of the parameters that rule the *a priori* distributions of $\boldsymbol{R}$ and the τ_ks, i.e., ν and q, respectively. Figs. 8 and 9 assume $N = 8$, $K = 8$, and a nominal value of P_{fa} equal to 10^{-3}; the number of Monte Carlo runs is 10^6. In Fig. 8 we plot the P_{fa}, obtained using the thresholds estimated assuming a nominal value of $\nu = 10$, versus the actual ν. In Fig. 9, instead, we plot the P_{fa}, obtained using the thresholds estimated assuming a nominal value of $q = 4$, versus

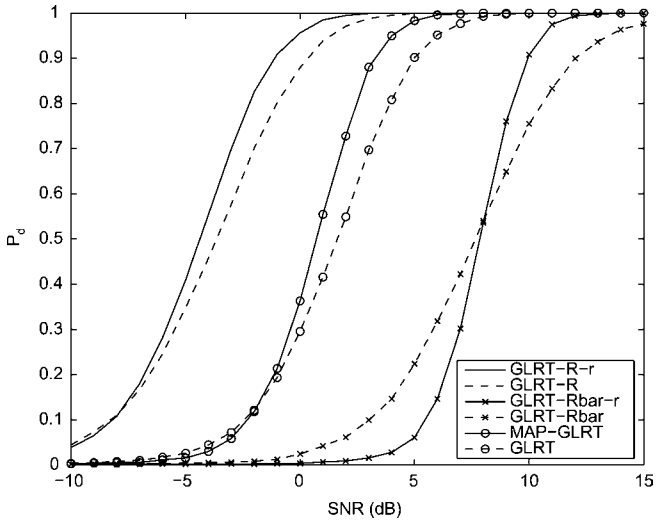

Fig. 6. P_d versus SNR for the considered detectors: $N = 8$, $K = 8$, $N_t = 2$, $\nu = 10$, $q = \beta = 4$, $P_{fa} = 10^{-3}$.

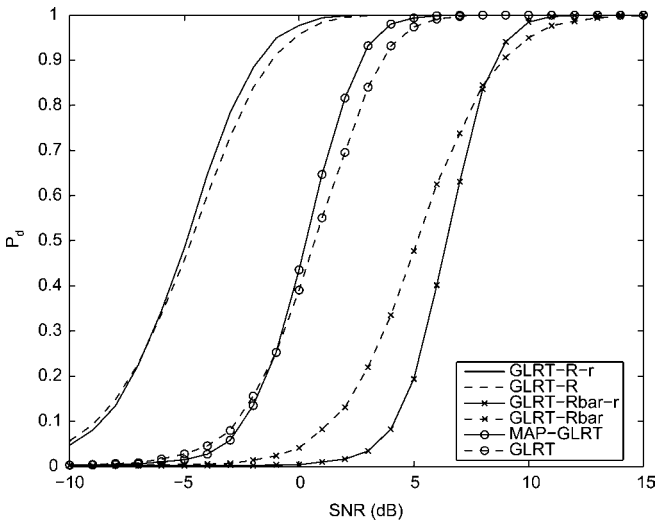

Fig. 7. P_d versus SNR for the considered detectors: $N = 8$, $K = 8$, $N_t = 4$, $\nu = 10$, $q = \beta = 4$, $P_{fa} = 10^{-3}$.

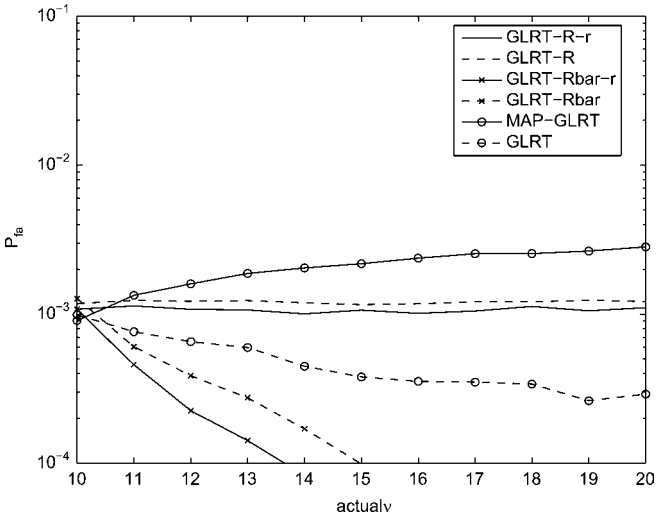

Fig. 8. P_{fa} versus ν for the considered detectors: $N = 8, K = 8, q = \beta = 4$, thresholds set assuming $\nu = 10$, $P_{fa} = 10^{-3}$.

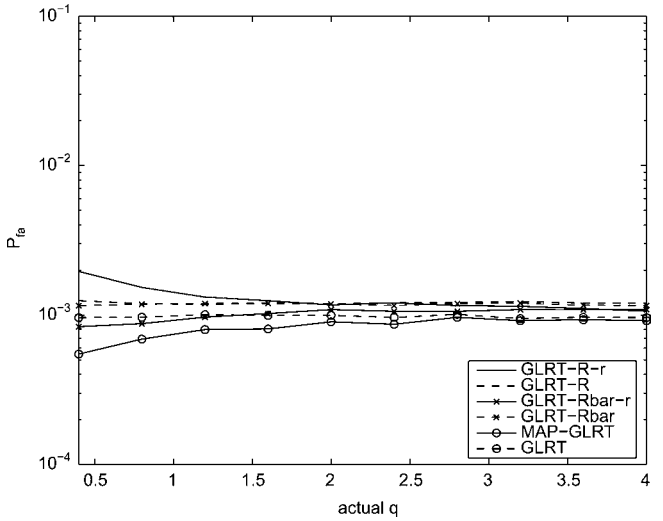

Fig. 9. P_{fa} versus q for the considered detectors: $N = 8$, $K = 8$, $\nu = 10$, thresholds set assuming $q = \beta = 4$, $P_{fa} = 10^{-3}$.

the actual q. Inspection of the figures highlights that the sensitivity with respect to ν of the proposed detectors (i.e., those marked with "o") remains less than one order of magnitude; as to the sensitivity with respect to q, it is evident from the figure that such a parameter basically does not affect the actual P_{fa}.

Finally, we have also studied the effect on the performance of an imperfect knowledge of the average matrix $\bar{\boldsymbol{R}}$. To this end, we have assumed that $\bar{\boldsymbol{R}}$ is estimated from a window of K_S heterogeneous independent data, say $\boldsymbol{r}_1, \ldots, \boldsymbol{r}_{K_S}$. Specifically, we have considered two different statistical models for the $\boldsymbol{r}_k$s

- Model A: the $\boldsymbol{r}_k$s, given the τ_ks and $\boldsymbol{R}_S$, are independent $\mathcal{CN}_N(\boldsymbol{0}, \tau_k \boldsymbol{R}_S)$, with $\tau_k \sim \mathcal{G}(q, \beta)$, $\boldsymbol{R}_S \sim \mathcal{CW}^{-1}\left((\nu - N)\bar{\boldsymbol{R}}, \nu\right)$, and the τ_ks and $\boldsymbol{R}_S$ independent random quantities;
- Model B: the $\boldsymbol{r}_k$s, given the $\boldsymbol{R}_k$s, are independent $\mathcal{CN}_N(\boldsymbol{0}, \boldsymbol{R}_k)$, with $\boldsymbol{R}_k \sim \mathcal{CW}^{-1}\left((\nu - N)\bar{\boldsymbol{R}}, \nu\right)$, and the $\boldsymbol{R}_k$s independent random matrices,

and set

$$\hat{\bar{\boldsymbol{R}}} = \frac{1}{K_S} \sum_{k=1}^{K_S} \boldsymbol{r}_k \boldsymbol{r}_k^{\dagger}.$$

In Figs. 10 and 11, we present results of P_d versus SNR for Model A and Model B, respectively, with $K_S = 16$; as to the remaining parameters, we have chosen $N = 8, K = 8, \nu = 10$, $q = \beta = 4$, $P_{fa} = 10^{-3}$. Moreover, thresholds have been estimated according to the selected (either A or B) Model. From Fig. 10 it is seen that the gain of GLRT and MAP-GLRT with respect to GLRT-$\bar{\boldsymbol{R}}$-r and GLRT-$\bar{\boldsymbol{R}}$ is reduced to about 1 dB. In Fig. 11, instead, we can see that GLRT and MAP-GLRT still guarantee a significant gain with respect to their competitors, as observed in Fig. 4.

Summarizing, the proposed detectors are rather robust to mismatches between nominal and operating conditions, at least for the considered parameters values.

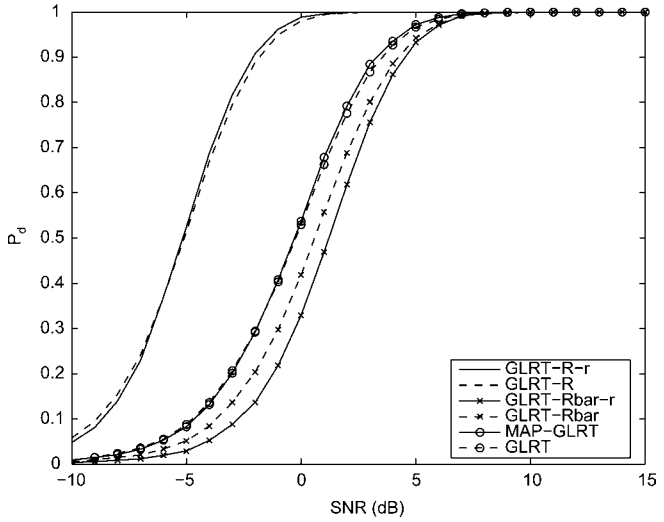

Fig. 10. P_d versus SNR for the considered detectors: $N = 8, K = 8, \nu = 10$, $q = \beta = 4$, $\bar{\boldsymbol{R}}$ estimated according to Model A, $K_S = 16$, $P_{fa} = 10^{-3}$.

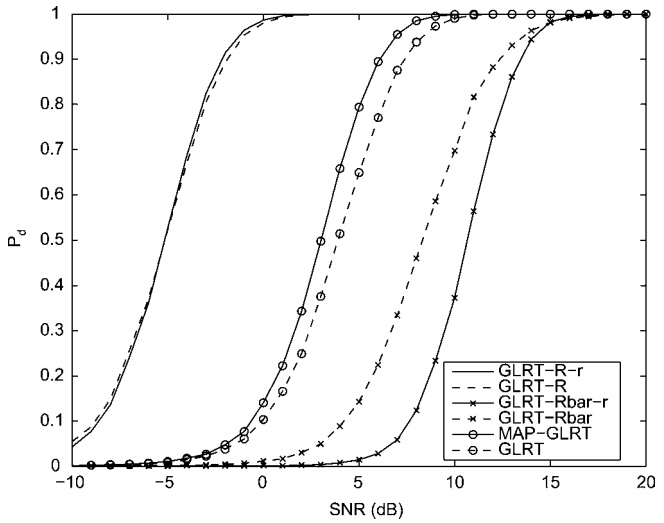

Fig. 11. P_d versus SNR for the considered detectors: $N = 8, K = 8, \nu = 10$, $q = \beta = 4$, $\bar{\boldsymbol{R}}$ estimated according to Model B, $K_S = 16$, $P_{fa} = 10^{-3}$.

V. Conclusion

In this paper, we have dealt with adaptive detection of distributed targets embedded in colored noise modeled in terms of a compound-Gaussian process and without assuming that a set of secondary data is available. The covariance matrices of the data under test share a common structure while having different power levels. A Bayesian approach has been pursued where the structure of the clutter covariance matrix and possibly the power levels are assumed to be random, with appropriate distributions. Within this framework GLRT-based and *ad-hoc* detectors have been designed. Some simulation studies have been presented to illustrate the performances of the proposed algorithms. The analysis indicates that the Bayesian framework could be a viable means to get rid of secondary data in heterogeneous scenarios. In particular, it is shown that GLRT and MAP-GLRT can outperform GLRT-$\bar{\boldsymbol{R}}$ and GLRT-$\bar{\boldsymbol{R}}$-r detectors and that, in presence of an informative pdf for the texture, MAP-GLRT has better performance than the GLRT.

References

[1] E. J. Kelly and K. Forsythe, "Adaptive detection and parameter estimation for multidimensional signal models," Lincoln Lab., Mass. Inst. Technol., Lexington, Tech. Rep. 848, 1989.

[2] E. Conte, A. De Maio, and G. Ricci, "GLRT-based adaptive detection algorithms for range-spread targets," *IEEE Trans. Signal Process.*, vol. 49, no. 7, pp. 1336–1348, Jul. 2001.

[3] L. T. McWhorter, "A high resolution detector in multi-path environments," in *Proc 12th Ann. Workshop on Adaptive Sensor Array Process. (ASAP), Lincoln Lab., MIT*, Lexington, MA, Mar. 16–18, 2004.

[4] F. Bandiera, A. De Maio, A. S. Greco, and G. Ricci, "Adaptive radar detection of distributed targets in homogeneous and partially homogeneous noise plus subspace interference," *IEEE Trans. Signal Process.*, vol. 55, no. 4, pp. 1223–1237, Apr. 2007.

[5] F. Bandiera, O. Besson, D. Orlando, G. Ricci, and L. L. Scharf, "GLRT-based direction detectors in homogeneous noise and subspace interference," *IEEE Trans. Signal Process.*, vol. 55, no. 6, pt. 1, pp. 2386–2394, Jun. 2007.

[6] K. D. Ward, C. J. Baker, and S. Watts, "Maritime surveillance radar. Part 1: Radar scattering from the ocean surface," *Inst. Elect. Eng. Proc. F*, vol. 137, no. 2, pp. 51–62, 1990.

[7] A. Farina, F. Gini, M. V. Greco, and L. Verrazzani, "High resolution sea clutter data: Statistical analysis of recorded live data," *Inst. Elect. Eng. Proc.-Radar, Sonar Navig.*, vol. 144, no. 3, pp. 121–130, Jun. 1997.

[8] E. Conte, M. Di Bisceglie, C. Galdi, and G. Ricci, "A procedure for measuring the coherence length of the sea texture," *IEEE Trans. Instrum. Meas.*, vol. 46, pp. 836–841, Aug. 1997.

[9] E. Conte, A. De Maio, and C. Galdi, "Statistical analysis of real clutter at different range resolutions," *IEEE Trans. Aerosp. Electron. Syst.*, vol. 40, no. 3, pp. 903–918, Jul. 2004.

[10] K. J. Sangston and K. R. Gerlach, "Coherent detection of radar targets in a non-Gaussian background," *IEEE Trans. Aerosp. Electron. Syst.*, vol. 30, no. 2, pp. 330–340, Apr. 1994.

[11] M. Di Bisceglie and C. Galdi, "Random walk based characterization of radar backscatter from the sea surface," *Inst. Elect. Eng. Proc.-Radar, Sonar Navig.*, vol. 145, no. 4, pp. 216–225, 1998.

[12] E. Conte and M. Longo, "Characterisation of radar clutter as a spherically invariant process," *Inst. Elect. Eng. Proc. F*, vol. 134, no. 2, pp. 191–197, Apr. 1987.

[13] E. Conte, M. Longo, and M. Lops, "Modeling and simulation of non-Rayleigh radar clutter," *Inst. Elect. Eng. Proc. F*, vol. 138, no. 2, pp. 121–130, 1991.

[14] M. Rangaswamy, D. Weiner, and A. Ozturk, "Computer generation of correlated non-Gaussian radar clutter," *IEEE Trans. Aerosp. Electron. Syst.*, vol. 31, no. 1, pp. 106–116, Jan. 1995.

[15] K. Gerlach, "Spatially distributed targets detection in non-Gaussian clutter," *IEEE Trans. Aerosp. Electron. Syst.*, vol. 35, no. 3, pp. 926–934, Jul. 1999.

[16] E. Conte, A. De Maio, and G. Ricci, "CFAR detection of distributed targets in non-Gaussian disturbance," *IEEE Trans. Aerosp. Electron. Syst.*, vol. 38, no. 2, pp. 612–621, Apr. 2002.

[17] R. Klemm, "Principles of space-time adaptive processing," *IEE Radar, Sonar, Navig. Avion. Series 12*, 2002.

[18] W. L. Melvin, "Space-time adaptive radar performance in heterogeneous clutter," *IEEE Trans. Aerosp. Electron. Syst.*, vol. 36, no. 2, pp. 621–633, Apr. 2000.

[19] D. J. Rabideau and A. O. Steinhardt, "Improving the performance of adaptive arrays in nonstationary environments through data-adaptive training," in *Proc. 30th Asilomar Conf. Signals Syst. Comput.*, Pacific Grove, CA, Nov. 3–6, 1996, pp. 75–79.

[20] D. J. Rabideau and A. O. Steinhardt, "Improved adaptive clutter cancellation through data-adaptive training," *IEEE Trans. Aerosp. Electron. Syst.*, vol. 35, no. 3, pp. 879–891, Jul. 1999.

[21] W. L. Melvin and M. C. Wicks, "Improving practical space-time adaptive radar," in *Proc. IEEE Nat. Radar Conf.*, May 13–15, 1997, pp. 48–53.

[22] K. Gerlach, S. D. Blunt, and M. L. Picciolo, "Robust adaptive matched filtering using the FRACT algorithm," *IEEE Trans. Aerosp. Electron. Syst.*, vol. 40, no. 3, pp. 929–945, Jul. 2004.

[23] M. Rangaswamy, "Statistical analysis of the nonhomogeneity detector for non-Gaussian interference backgrounds," *IEEE Trans. Signal Process.*, vol. 53, no. 6, pp. 2101–2111, Jun. 2005.

[24] K. Gerlach and M. J. Steiner, "Adaptive detection of range distributed targets," *IEEE Trans. Signal Process.*, vol. 47, no. 7, pp. 1844–1851, Jul. 1999.

[25] F. Bandiera, D. Orlando, and G. Ricci, "CFAR detection of extended and multiple point-like targets without assignment of secondary data," *IEEE Signal Process. Lett.*, vol. 13, no. 4, pp. 240–243, Apr. 2006.

[26] F. Bandiera and G. Ricci, "Adaptive detection and interference rejection of multiple point-like radar targets," *IEEE Trans. Signal Process.*, vol. 54, no. 12, pp. 4510–4518, Dec. 2006.
[27] G. Alfano, A. De Maio, and A. Farina, "Model-based adaptive detection of range-spread targets," *Inst. Elect. Eng. Proc.-Radar Sonar Navig.*, vol. 151, no. 1, pp. 2–10, Feb. 2004.
[28] F. Bandiera, M. Guerriero, and G. Ricci, "Optimized algorithms for detection of sparse targets in heterogeneous Gaussian noise," in *Proc. Int. Radar Conf. 2009*, Bordeaux, France, Oct. 12–16, 2009.
[29] F. Bandiera, D. Orlando, G. Ricci, and L. L. Scharf, "Radar detection of a swerling 2 pulse train in clutter plus thermal noise: A subspace identification approach," in *Proc. 2nd Int. Workshop on Cognitive Inf. Process.* , Elba Island, Italy, Jun. 14–16, 2010.
[30] "Knowledge-based systems for adaptive radar: Detection, tracking and classification," *IEEE Signal Process. Mag., Special Issue*, Jan. 2006.
[31] J. R. Guerci and E. J. Baranoski, "Knowledge-aided adaptive radar at DARPA-an overview," *IEEE Signal Process. Mag.*, vol. 23, no. 1, pp. 41–50, Jan. 2006.
[32] in *KASSPER Workshops, 2002-2005* [Online]. Available: http://www.darpa.mil/spo/programs/kassper.htm
[33] J. S. Bergin, C. M. Teixeira, P. M. Techau, and J. R. Guerci, "Spacetime beamforming with knowledge-aided constraints," in *Proc 11th Adapt. Sens. Array Process. Workshop*, Lexington, MA, Mar. 11–12, 2003.
[34] J. S. Bergin, C. M. Teixeira, P. M. Techau, and J. R. Guerci, "STAP with knowledge-aided data prewhitening," in *Proc. IEEE Radar Conf.*, Philadelphia, PA, Apr. 26–29, 2004, pp. 289–294.
[35] K. Gerlach and M. L. Picciolo, "Airborne/spacebased radar STAP using a structured covariance matrix," *IEEE Trans. Aerosp. Electron. Syst.*, vol. 39, no. 1, pp. 269–281, Jan. 2003.
[36] W. L. Melvin and J. R. Guerci, "Knowledge-aided signal processing: A new paradigm for radar and other advanced sensors," *IEEE Trans. Aerosp. Electron. Syst.*, vol. 42, no. 3, pp. 983–996, Jul. 2006.
[37] E. Conte, A. De Maio, A. Farina, and G. Foglia, "Design and analysis of a knowledge-aided radar detector for Doppler processing," *IEEE Trans. Aerosp. Electron. Syst.*, vol. 42, no. 3, pp. 1058–1079, Jul. 2006.
[38] A. De Maio, A. Farina, and G. Foglia, "Design and experimental validation of knowledge-based constant false alarm rate detectors," *IET Radar, Sonar, Navig.*, vol. 1, no. 4, pp. 308–316, Aug. 2007.
[39] A. De Maio, S. De Nicola, L. Landi, and A. Farina, "Knowledge-aided covariance matrix estimation: A Maxdet approach," *IET Radar, Sonar, Navig.*, vol. 3, no. 4, pp. 341–356, Aug. 2009.
[40] A. De Maio and A. Farina, "Adaptive radar detection: A Bayesian approach," in *Proc. Int. Radar Symp. (IRS)* , May 24–26, 2006, pp. 1–4.
[41] A. De Maio, A. Farina, and G. Foglia, "Adaptive radar detection: A Bayesian approach," in *Proc. IEEE Radar Conf.*, Apr. 17–20, 2007, pp. 624–629.
[42] O. Besson, J.-Y. Tourneret, and S. Bidon, "Knowledge-aided Bayesian detection in heterogeneous environments," *IEEE Signal Process. Lett.*, vol. 14, no. 5, pp. 355–358, May 2007.
[43] S. Bidon, O. Besson, and J.-Y. Tourneret, "A Bayesian approach to adaptive detection in non-homogeneous environments," *IEEE Trans. Signal Process.*, vol. 56, no. 1, pp. 205–217, Jan. 2008.
[44] O. Besson, S. Bidon, and J.-Y. Tourneret, "Covariance matrix estimation with heterogeneous samples," *IEEE Trans. Signal Process.*, vol. 56, no. 3, pp. 909–920, Mar. 2008.
[45] F. Bandiera, O. Besson, and G. Ricci, "Knowledge-aided covariance matrix estimation and adaptive detection in compound-Gaussian noise," *IEEE Trans. Signal Process.*, vol. 58, no. 10, pp. 5390–5396, Oct. 2010.
[46] F. Bandiera, O. Besson, and G. Ricci, "Covariance-informed detection in compound-Gaussian clutter without secondary data," in *Proc. 6th IEEE Sens. Array and Multichannel Signal Process. Workshop*, Israel, Oct. 4–7, 2010.
[47] J. Ward, "Space-time adaptive processing for airborne radar," Lincoln Lab., Mass. Instit. Technol., Lexington, Tech. Rep. 1015, 1994.
[48] J. S. Bergin, C. M. Teixeira, P. M. Techau, and J. R. Guerci, "Improved clutter mitigation performance using knowledge-aided space-time adaptive processing," *IEEE Trans. Aerosp. Electron. Syst.*, vol. 42, no. 3, pp. 997–1009, Jul. 2006.
[49] J. D. Hiemstra, "Colored diagonal loading," in *Proc. IEEE Radar Conf.*, Apr. 22–25, 2002, pp. 386–390.
[50] E. Conte, A. De Maio, and G. Ricci, "Recursive estimation of the covariance matrix of a compound Gaussian process and its application to adaptive CFAR detection," *IEEE Trans. Signal Process.*, vol. 50, no. 8, pp. 1908–1915, Aug. 2002.
[51] M. S. Greco and F. Gini, "Covariance matrix estimation for CFAR detection in correlated heavy tailed clutter," *Signal Process.*, vol. 82, no. 12, pp. 1847–1859, Dec. 2002.
[52] E. Conte and A. De Maio, "Mitigation techniques for non-Gaussian sea clutter," *IEEE J. Ocean. Eng.* , vol. 29, no. 2, pp. 284–302, Apr. 2004.
[53] F. Pascal, Y. Chitour, J.-P. Ovarlez, P. Forster, and P. Larzabal, "Covariance structure maximum-likelihood estimates in compound Gaussian noise: Existence and algorithm analysis," *IEEE Trans. Signal Process.*, vol. 56, no. 1, pp. 34–48, Jan. 2008.
[54] E. Conte, M. Lops, and G. Ricci, "Asymptotically optimum radar detection in compound-Gaussian clutter," *IEEE Trans. Aerosp. Electron. Syst.*, vol. 31, no. 2, pp. 617–625, Apr. 1995.
[55] I. F. Gradshteyn and I. M. Ryzhik, *Table of Integrals, Series, and Products*, Fifth ed. New York: Academic, 1994.
[56] E. Conte, M. Longo, M. Lops, and S. L. Ullo, "Radar detection of signals with unknown parameters in K-distributed clutter," *IET Proc. Radar Signal Process.—Part F*, vol. 138, no. 2, pp. 131–138, Apr. 1991.
[57] M. Abramowitz and I. A. Stegun, *Handbook of Mathematical Functions with Formulas, Graph, and Mathematical Tables*. New York: Dover, 1972.

Francesco Bandiera (M'01) was born in Maglie (Lecce), Italy, on March 9, 1974. He received the Dr. Eng. degree in computer engineering and the Ph.D. degree in information engineering from the University of Lecce (now University of Salento), Italy, in 2001 and 2005, respectively.

From July 2001 to February 2002, he was with the University of Sannio, Benevento, Italy, engaged in a research project on mobile cellular telephony. Since December 2004, he has been an Assistant Professor with the Dipartimento di Ingegneria dell'Innovazione, University of Salento, Lecce, where he is engaged in teaching and research. The main research interests are in the field of statistical signal processing with focus on radar signal processing, multiuser communications, and pollution detection on the sea surface based upon SAR imagery. He has held visiting positions with the Electrical and Computer Engineering Department, University of Colorado at Boulder, (September 2003-March 2004), and with the Department of Avionics and Systems of ENSICA [now Institut Supérieur de l'Aéronautique et de l'Espace (ISAE)], Toulouse, France (October 2006).

Olivier Besson (S'90–M'93–SM'04) received the M.Sc. degree in signal processing in 1988 and the Ph.D. degree in signal processing in 1992, both from the National Polytechnic Institute of Toulouse.

He is currently a Professor with the Institut Supérieur de l'Aéronautique et de l'Espace (ISAE), Toulouse, France. His research interests are in the area of robust statistical array processing with main application in radar.

Dr. Besson is a former Associate Editor for the IEEE TRANSACTIONS ON SIGNAL PROCESSING and the IEEE SIGNAL PROCESSING LETTERS. He is currently a member of the Sensor Array and Multichannel (SAM) Technical Committee of the IEEE Signal Processing Society.

Giuseppe Ricci (M'01–SM'10) was born in Naples, Italy, on February 15, 1964. He received the Dr. degree and the Ph.D. degree, both in electronic engineering, from the University of Naples "Federico II" in 1990 and 1994, respectively.

Since 1995, he has been with the University of Salento (formerly University of Lecce), Italy, first as an Assistant Professor of Telecommunications and, since 2002, as a Professor. His research interests are in the field of statistical signal processing with emphasis on radar processing and CDMA systems. More precisely, he has focused on high-resolution radar clutter modeling, detection of radar signals in Gaussian and non-Gaussian disturbance, oil spill detection from SAR data, track-before-detect algorithms fed by space-time radar data, multiuser detection in overlay CDMA systems, and blind multiuser detection. He has held visiting positions with the University of Colorado at Boulder during 1997–1998 and April/May 2001; with Colorado State University during July/September 2003, March 2005, September 2009, and March 2011; with Ensica (Toulouse, France) in March 2006; and with the University of Connecticut, Storrs, in September 2008.